Contents list available at CBIORE journal website

International Journal of Renewable Energy Development

Journal homepage: https://ijred.cbiore.id

Research Article

Electrical performance for in-situ doping of phosphorous in silver paste screen-printed contact on p-type silicon solar cell

Nurul Aqidah Mohd Sinin[a*], Ahmad Rujhan Mohd Rais[b*], Zon Fazlila Mohd Ahir[c], Kamaruzzaman Sopian[a,d], Mohd Adib Ibrahim[a*]

[a]*Solar Solar Energy Research Institute, Universiti Kebangsaan Malaysia, 43600 Bangi, Selangor, Malaysia*

[b]*School of Physics, Universiti Sains Malaysia, 11800 USM Penang, Malaysia*

[c]*Faculty of Technical and Vocational, Universiti Pendidikan Sultan Idris, 35900 Tanjung Malim, Perak Darul Ridzuan, Malaysia*

[d]*Mechanical Engineering, Department of Mechanical Engineering, Universiti Teknologi PETRONAS, 32610 Seri Iskandar, Perak Darul Ridzuan, Malaysia*

Abstract. This study addresses the challenge of enhancing the efficiency of silicon solar cells by investigating the electrical performance of phosphorus-doped silver (Ag-P) pastes used in screen-printed contacts on p-type silicon wafers. Conventional silver (Ag) pastes serve as conductive contacts but lack the ability to simultaneously doped the emitter region, leading to complex fabrication processes and limiting cell efficiency. To overcome this, we explore an in-situ approach using Ag-based paste and phosphoric acid (H_3PO_4), which combines emitter doping and contact formation, thereby simplifying fabrication while enhancing performance. In this study, both un-doped and phosphorus-doped Ag pastes were screen-printed onto planar, textured, and silicon dioxide-passivated silicon wafers, followed by annealing at 900°C by using a round quartz tube furnace with 45s in and 45s out with a holding time of the 40s. Electrical performance was measured through light-current-voltage (LIV) and quantum efficiency analyses. According to the short circuit current density (J_{SC}) for only Ag-based paste screen-printed on only one-sided (A) and both-sided (B) indicates a higher J_{SC} value of 9.63 mA/cm^2 for A meanwhile, sample B gains 7.54 mA/cm^2. For comparison, the J_{SC} values for screen-printed Ag-P on only one side (A) and both sides (B) are 10.4 mA/cm^2 and 10.4 mA/cm^2, respectively. Thus, the overall efficiency of Ag-P screen-printed on a one-sided Si wafer was 1.65% higher than that of the rest of the samples. However, the internal quantum efficiency (IQE) and external quantum efficiency (EQE) for Ag-P screen-printed on Si wafer display higher percentages between 80-83% and 63-73% at a wavelength range of 650 to 900 nm than the rest of the samples. The QE measurements reveal that Ag-P paste effectively mitigates surface recombination losses, resulting in higher efficiency and improved charge carrier collection. These findings indicate that Ag-P paste offers a viable alternative to conventional screen-printed contacts by enhancing both device performance and electrical efficiency through integrated doping and contact formation. This work suggests that Ag-P paste could play a vital role in advancing high-performance silicon solar cell technologies.

Keywords: electrical performance, light-current-voltage, phosphorus-doped, quantum efficiency, silver-based pastes

Received: 11th Nov 2024; Revised: 19th May 2025; Accepted: 1st June 2025; Available online: 15th June 2025

1. Introduction

The photovoltaic industry plays a crucial role in the global energy landscape (Abid *et al*., 2023; Andreani *et al*., 2019; Y. Zhou, 2013) competing with renewable and conventional energy sources. Crystalline silicon (c-Si) (Goodrich *et al*., 2013; Lan *et al*., 2015; Sopian *et al*., 2017) wafer-based technologies dominate the photovoltaic market for terrestrial applications due to their high efficiency, stability, and technological advancements leveraged from the microelectronics industry. However, the high production costs of c-Si solar cells necessitate continuous research aimed at developing low-cost alternatives without compromising performance. The fabrication (Battaglia *et al*., 2016; Sui *et al*., 2021) of silicon solar cells involves several key steps, such as surface texturing (Basher *et al*., 2019; Kim *et al*., 2020; Mohd Rais *et al*., 2022), emitter diffusion (n^+ and p^+ regions) (Li *et al*., 2017; Mohd Ahir *et al*., 2018; Sheng *et al*., 2019), anti-reflection coatings (ARC) (Akter *et al*., 2022; L. Zhou *et al*., 2018), and contact metallization (Oh *et al*., 2019; Sepeai *et al*., 2011; Shanmugam *et al*., 2014; Wu *et al*., 2017). These processes play a pivotal role in determining crucial electrical parameters such as open-circuit voltage (V_{OC}), short-circuit current density (J_{SC}), and fill factor (FF), all of which are influenced by specific fabrication conditions. Although conventional Si processing technology is well-established, continuous modification of fabrication techniques and device structure remains necessary to further improve the electrical performance of solar cells.

Currently, most photovoltaic manufacturers use boron-doped p-type wafers to fabricate c-Si solar cells. Figure 1 shows the conventional fabrication process of silicon solar cells. As

* Corresponding author(s)
Email: nurulaqidah88@mail.com (N. A. M. Sinin); mdadib@ukm.edu.my (M.A. Ibrahim) ; rujhanrais@usm.my (A. R. M. Rais)

https://doi.org/10.61435/ijred.2025.60822
ISSN: 2252-4940/© 2025.The Author(s). Published by CBIORE

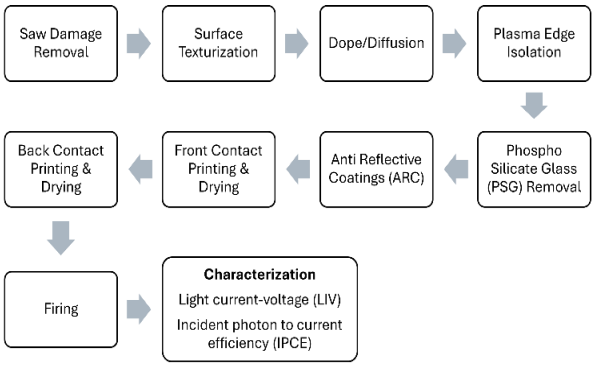

Fig 1 Schematic diagram of conventional fabrication process of silicon solar cell

noted in previous studies, each processing step in the conventional screen-printing solar cell contributes to certain losses. Despite process losses in traditional screen-printed cells, screen-printing technology remains a cost-competitive and robust approach due to advancements in printing media and the simplicity of the method.

Screen-printing technology has garnered considerable attention due to significant advancements in printing media and the simplicity of the process. This technology also enhances throughput and reduces production costs. While several alternatives to screen-printing exist for improving cell efficiency, the current screen-printing technology is more mature and cost-effective compared to newer methods which is widely implemented in fabricating Passivated Emitter and Rear Contact (PERC) (Lorenz *et al.*, 2018), Interdigitated Back Contact (IBC) (Chowdhury *et al.*, 2019), and Heterojunction (HIT) (C. Chen *et al.*, 2023). Consequently, approximately 85% of silicon solar cells are manufactured using screen printing of thick film pastes (Antoniadis, 2011; Lorenz *et al.*, 2018). In a typical solar cell manufacturing process, screen-printing has the potential to increase efficiency and reduce costs, particularly as metallization pastes continue to evolve, and new generations of pastes become available.

In the standard manufacturing process, silver (Ag) paste is screen-printed onto the front side of silicon wafers, while aluminum (Al) is applied and fired onto the rear to establish a conductive circuit. The front silver paste, serving as the electrode, plays a crucial role in optimizing the light conversion efficiency of silicon solar cells. The contact resistance between the Ag grid and the c-Si wafer is largely influenced by the glass system within the paste, which aids in etching or penetrating the ARC layer, thereby enhancing electrical connectivity (Yüce *et al.*, 2019). Additionally, the paste's composition is tailored to enable the printing of narrow grid lines with a high aspect ratio, minimizing shading losses and increasing the cell's exposed surface area for light absorption (Lee & Heo, 2017; Thibert *et al.*, 2014). Furthermore, functional additives in the paste, such as metal oxides and glass-modifying compounds, help form a low-resistance ohmic contact with the lightly doped silicon emitter, effectively reducing recombination losses and enhancing the cell's overall efficiency by improving charge carrier collection (Tepner *et al.*, 2021; Tepner & Lorenz, 2023).

In recent years, advancements in metallization pastes have sought to address the need for improved efficiency and cost reduction in silicon solar cells. Among these, phosphorus-doped silver (Ag-P) pastes have emerged as a promising alternative to traditional Ag pastes (Porter *et al.*, 2002; Rujhan *et al.*, 2024; Sinin *et al.*, 2023). By incorporating a phosphorus (P) dopant from phosphoric acid (H_3PO_4) into the Ag paste, this material serves as the conductive contact for the front electrode and enables simultaneous doping of the emitter region during the metallization process. This dual functionality reduces the complexity of cell fabrication by combining contact formation and emitter diffusion into a single step (Kulushich *et al.*, 2012; Zanesco *et al.*, 2019). The incorporation of P offers the potential for lower contact resistance and enhanced carrier collection, ultimately improving the electrical performance of the solar cells. As new generations of doped pastes are being explored, Ag-P paste presents an innovative approach to optimizing both the cost and efficiency of silicon solar cells.

Thus, this paper investigates the electrical performance of phosphorus-doped silver-based (Ag-P) paste as an alternative to conventional metallic dopant pastes. The formation of Ag-P paste is a combination of Ag paste with H_3PO_4. The Ag-P paste aims to simultaneously create the metallic contact and emitter region on the silicon wafer through an in-situ process. This involves the simultaneous diffusion of Ag and H_3PO_4 during screen printing, providing a potentially efficient and cost-effective method for solar cell fabrication.

2. Methodology

Several p-type single crystalline of (100) orientation was used. The samples were ±175 µm thick and had a resistivity of 0.5~3.0 Ω.cm respectively. The Si was cleaned by using a mixture of 10% of sodium hydroxide (NaOH) for 10 minutes and rinsed with deionized water. Then dipped into the mixture of hydrofluoric acid (HF) with distilled water (H_2O) with ratio of 1:50 (HF: H_2O) for 1 minutes and rinsed with deionized water to get a hydrophobic surface. The cleaned samples were divided into three categories, which are planar, textured and passivated wafers. For planar, the process was stopped until the hydrophobic surface. For textured wafers, the balanced of the planar wafers were textured in the solution of potassium hydroxide (KOH) mixed with hydrogen peroxide (H_2O_2) and distilled water (H_2O) with a ratio of 1:5:125 (KOH:H_2O_2:H_2O) for 30 minutes. Several textured wafers were passivated by depositing a thin layer of silicon oxide (SiO_2) using three stack furnaces at a higher temperature (921°C) for 45 minutes. Finally, the metallization processes were carried out using

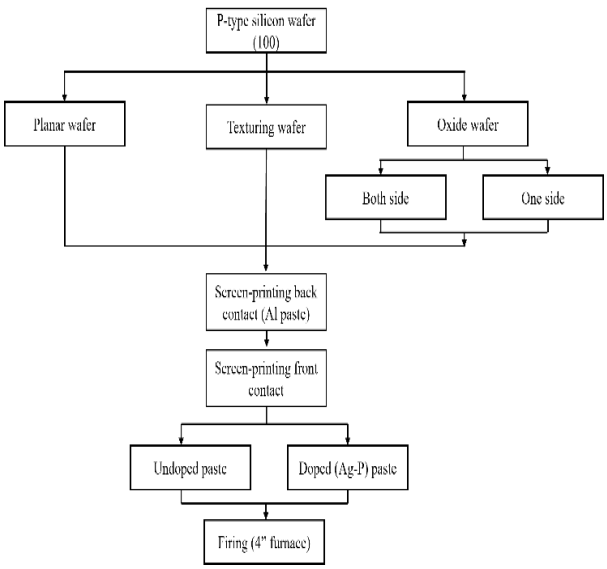

Fig 2 Summarized process of in-situ doping of Phosphorous in Silver paste Screen-printed Contact on Silicon Solar Cell

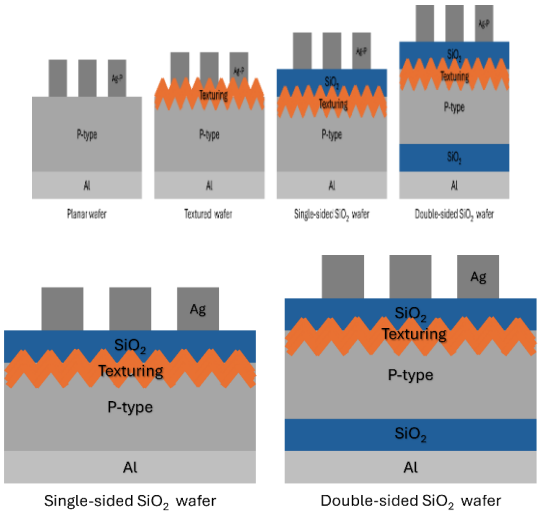

Fig 3 Structure of planar, textured and passivated of silicon wafer

screen-printing of silver (Ag) and aluminium (Al) pastes by employing identical grid masks on the front and back surfaces. Two types of Ag pastes were used, which are Ag-based (undoped) paste and phosphorus-doped Ag-based, known as Ag-P paste. The formation of Ag-P paste is a combination of silver paste with phosphoric acid (H_3PO_4) (Meier *et al*., 2000; Rujhan *et al*., 2024; Shanmugam *et al*., 2016; Sinin *et al*., 2023). The Ag paste weight of 10 mg is mixed with a variation of percentage H_3PO_4solution as a dopant source. The mixture is swirled constantly for 5 min to make sure it is well mixed. 10% Ag/P paste is the most compromising to be used as dopant paste for both n-type and p-type wafers with different annealing times (40 sec, 20 sec), respectively, due to its improvement from semi-ohmic to ohmic behaviour and well-annealed together in in-situ process on the Si wafer (Sinin *et al*., 2023). The samples were subsequently annealed at 900°C by using a quartz tube furnace with 45s in and 45s out with a holding time of the 40s. The electrical performance of the silicon solar cells was measured using light-current-voltage measurement to find the efficiency, and incident-photon-to-current-efficiency (IPCE) measurement was used to measure the external and internal quantum efficiency of the cells. Figure 2 summarises all the processes involved in this paper while Figure 3 illustrated the structure for each wafer along this fabrication process.

3. Results and Discussion

3.1 Microstructure and Morphology

Past research by Sinin et al. (Sinin *et al*., 2023) optimizes the concentration factor on the mixture of silver (Ag) paste and phosphoric acid (H_3PO_4) solution as a dopant paste for contact

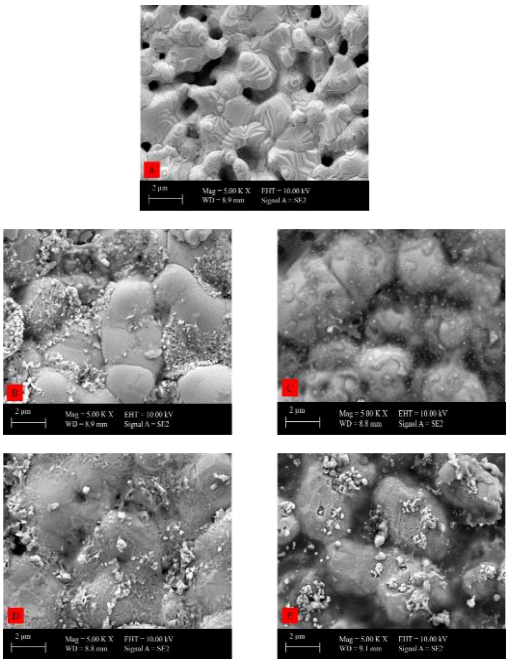

Fig 4 FESEM top view image of (A) reference (Ag-based paste), (B) 5% of Ag/P for 10s annealing, (C) 5% of Ag/P for 40s annealing, (D) 10% of Ag/P for 10s annealing and (E) 10% of Ag/P for 40s annealing

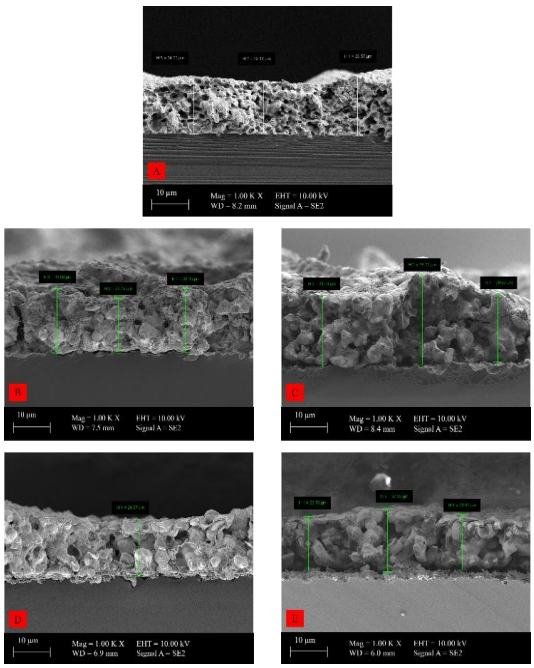

Fig 5 FESEM cross-section images of (A) reference (Ag-based paste), (B) 5% of Ag/P for 10s annealing, (C) 5% of Ag/P for 40s annealing, (D) 10% of Ag/P for 10s annealing and (E) 10% of Ag/P for 40s annealing

formation in silicon solar cells. The morphology and topography of the phosphorus-doped silver (Ag-P) paste concentration were investigated using Field Emission Scanning Electron Microscopy (FESEM).

Figure 4 shows the topography view images from FESEM for reference (Ag-based) sample and Ag-P (5% and 10%) on p-type silicon (p-Si) wafers for 10s and 40s respectively. According to Figure 4 (a), the adjoining particles from Ag paste fuse together and agglomerate into bunches for reference (A) sample. Other than that, the dopant paste of Ag-P exhibits a lot of H_3PO_4 excess in the surface due to shorter time for annealing process for 5% Ag-P paste as shown in Figure 4(b). Meanwhile, Figure 4 (c) shows a better diffusion of H_3PO_4 on Ag paste as the distribution of the larger phosphorous (P) precipitate has been reduced and well diffused as compared with 5% Ag-P Based on Figure 4(d), less concentration of P precipitates for 10% Ag-P than 5% Ag-P appears on p-Si due to a more uniform formation of a higher percentage of P mixed with Ag paste when annealed with the same time taken. Meanwhile, Figure 4(e) shows a well distribution of P as the combination of Ag-P paste annealed at longer duration makes the metallic dopant paste more uniform and there are no hollows shown as compared with Figure 4(c) and (d). This is due to the reaction between Ag and P at high temperature and longer duration will make the Ag-P paste melt more melted and make the metallic dopant paste automatically fill the hollow as shown in Figure (d).

Figure 5 exhibit the cross section for the Ag-based and Ag-P with different concentration (5% and 10%) at different holding time (10s and 40s) during annealing process. According to Figure 5 (b), (c), (d), and (e), the Ag-P pastes were melted and filled the hollow gaps between Ag-based, as shown in Figure 5(a). Besides that, Figure 5 (e) exhibits a denser Ag-P dopant paste than the rest of the concentration Ag-P and the annealing time taken. Thus, 10% of Ag-P paste were selected with annealing time of 40s to be used throughout this experiment to investigate the electrical performance. A higher Ag-P concentration (10%) and longer annealing time (40s) resulted in better diffusion, densification, and improved contact formation, reducing voids and enhancing conductivity. Therefore, 10% Ag-P with 40s annealing was selected to optimize electrical performance in the experiment.

3.2 Current-Voltage (I-V) Measurement

In silicon solar cells, to enhance more incident light being absorbed on the front surface, the anti-reflection coating-like passivation layer from a thermally grown silicon oxide thin layer has been created (Zhang *et al.*, 2019). In this experiment, the wafers were coated with a thin layer of silicon oxide (SiO_2) in a three-stack furnace at a higher temperature of 900-1000°C for 45 minutes. This process is known as the wet process of thermal oxide diffusion. Normally, the layer will deposit on both sides, but, in this experiment, we remove one side layer of SiO_2 of several wafers by using vapour method from vapour produced from hydrofluoric acid (HF) solution until the layer is totally removed (surface becomes hydrophobic).

The interfacial oxide, specifically the thermally grown SiO_2 layer, interacting with the emitter and metallic base contacts introduces challenges for charge carriers. This oxide reduces interface traps, which can otherwise negatively influence the Fermi level's pinning at the surface (Gaubert & Teramoto, 2017; Glatthaar *et al.*, 2022; Poncé *et al.*, 2020; Turkay *et al.*, 2019). A promising approach to enhance the open-circuit voltage (V_{OC}) is inserting an additional diffused region beneath the interfacial oxide layer (Glunz & Feldmann, 2018). The electrical performance of solar devices can vary significantly based on the type of SiO_2 coating applied. Specifically, devices with a SiO_2 coating only on the front surface tend to exhibit superior electrical performance compared to those that are fully coated with SiO_2 (Alamri *et al.*, 2020). Moreover, at elevated temperatures, the diffusion process can lead to a degradation in V_{OC}, maximum power output, and overall conversion efficiency (Savadogo *et al.*, 2020). This degradation is attributed to the

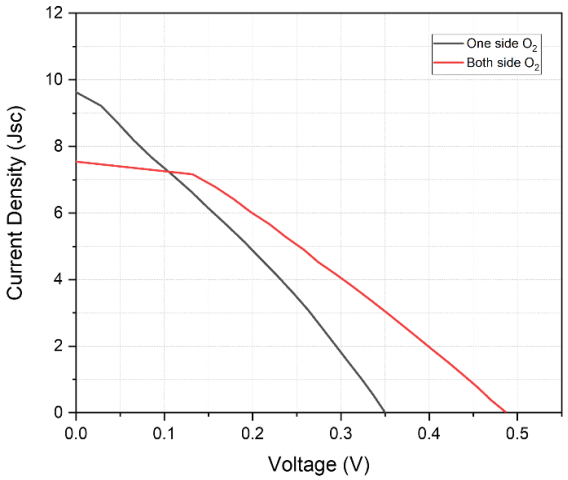

Fig 6 Current density - voltage evaluation for undoped Ag-based paste

reduction in silicon bulk carrier lifetime during high-temperature processing (Sui *et al.*, 2021).

Based on Figure 6, the Ag-based pastes were screen-printed on the planar wafer, textured wafer, doped wafer fully passivated and one-sided with SiO_2. For planar and textured wafers, there is no current-voltage graph due to due to the absence of an electric field and an emitter layer in the device (Dr. Alistair Proul, 2023; Eon *et al.*, 2018; Razeghi, 2009; Skromme, 2003). Based on performance variation, the curves indicate that the passivation significantly influences the electrical performance of the device. The one side O_2 layer (black curve) shows a steeper decline in current with increasing voltage compared to the sided O_2 layer (red curve), suggesting differences in carrier recombination rates. The red curve exhibits a relatively higher current density at most voltage levels, implying better charge carrier collection efficiency (Glunz & Feldmann, 2018; Zhuang *et al.*, 2019). This could be attributed to improved surface passivation, which reduces surface recombination losses (Y. L. Chen *et al.*, 2016; Rahman & Khan, 2012).

Figure 7 shows the electrical performance of phosphorus-doped Ag-based (Ag-P) paste on the planar wafer, textured wafer and passivated wafer. The short circuit current density (J_{sc}) for planar and textured wafers with Ag-P pastes will likely be low due to the absence of a p-n junction of a p-n junction, which is essential for generating a significant photo-current. Without this junction, there's no effective mechanism to separate electron-hole pairs, leading to minimal current generation. Textured wafers had intermediate performance, with J_{sc} of 3.33 mA/cm^2, indicating some degree of carrier collection but limited by higher surface recombination (Chaudhary *et al.*, 2021, 2022). The highest J_{sc} (10.4 mA/cm^2 was achieved on single-sided passivation wafers, likely due to enhanced carrier generation and collection afforded by the doping (Dou *et al.*, 2021).

The V_{oc} depends on the recombination rates and the quality of the p-n junction. In passivated wafer, we expect an increase in V_{oc} because passivation layers reduce recombination at the wafer surface, allowing for a higher buildup of carriers (Serenelli *et al.*, 2023; P. Yang *et al.*, 2013). This reduction in recombination directly contributes to a higher V_{oc}. The highest V_{oc} (0.533 V) was recorded for single-sided passivated wafers, suggesting that the combination of in-situ doping and passivation minimized recombination and allowed better carrier retention. Fully passivated wafers exhibited slightly lower V_{oc} (0.562 V), which might be due to the specific annealing conditions or interaction with both oxide layers. Due to the lack of p-n junction, planar and textured wafers are likely to have negligible V_{oc}, as they don't provide the electric field needed to sustain a potential difference, recorded very low V_{oc} of 0.028 V, as expected (Larionova *et al.*, 2017; Mandal *et al.*, 2020). The electron-hole pairs generated under illumination cannot contribute to a voltage build up effectively without a junction.

Table 1 represents the key performance for silicon solar cells using un-doped (Ag-based) paste and phosphorus-doped silver-based (Ag-P) paste under various wafers. For commercial samples, the values are robust, with a V_{oc} of 0.609 V, a high J_{sc} of 32.56 mA/cm^2, an FF of 0.656 and an efficiency of 13%. Comparing commercial and water-based H_3PO_4 as emitters on Si solar cells, both have different types of dopant sources and processes that will influence the overall performance of solar cells. The emitter formation based on 10% water-based H_3PO_4 was diffused on a Si wafer at 875ºC for 30 min, the same as the diffusion process of $POCl_3$ inside the quartz furnace. The overall performance of commercial Si solar cells is higher than water-based H_3PO_4. This is due to well established process of $POCl_3$ as an emitter as compared with the early stage of water-based H_3PO_4 as an emitter. The commercial cell outperforms the water-based H_3PO_4 cell across all parameters. It reveals that higher V_{OC} and J_{SC} for commercial silicon solar cells, indicating better charge carrier collection and low recombination losses. In addition, FF reflects lower resistive losses in commercial cells as compared with water-based H_3PO_4 cells. Thus, overall efficiency is higher for commercial cells suggesting that water-based H_3PO_4 as an open emitter for further process optimization in order to overcome commercial dopant sources.

Comparing experimental data with a commercial silicon solar cell provides a benchmark for performance evaluation. It helps identify efficiency gaps, validate new materials, and assess practical feasibility (Hamzavy & Bradley, 2013; Tripathi *et al.*, 2020). This comparison ensures scientific and industrial relevance, highlighting necessary optimizations while demonstrating progress toward achieving commercially viable solar cell technology. In contrast, the undoped Ag-based paste demonstrates lower V_{oc} and J_{sc} values, especially in the one-sided and both-sided oxide-passivated configurations. This reduction in performance highlights the limitations of undoped Ag paste in terms of charge carrier collection and surface passivation.

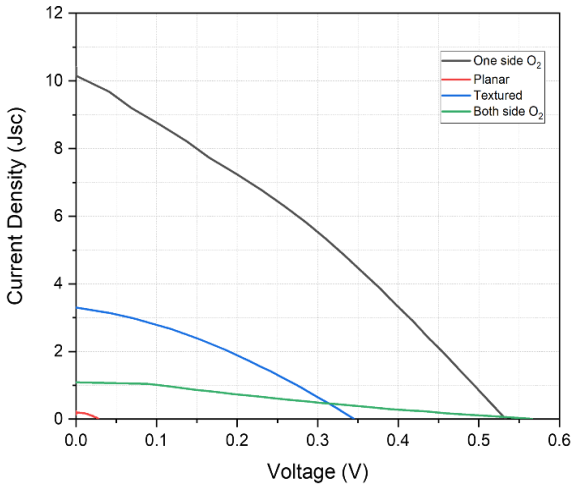

Fig 7 Current density - voltage evaluation for phosphorus-doped Ag-based (Ag-P) paste

Since planar and textured wafers lack a p-n junction, they will not generate a substantial photocurrent (current density, J_{sc}) under illumination. The absence of a depletion region means that electron-hole pairs do not separate effectively, leading to negligible current flow (Wurfel *et al*., 2015). Based on Table 1, passivated wafers (either full or one sided SiO_2) have a p-n junction, allowing them to generate significant photocurrent when exposed to light. Current density is generally higher in one-sided SiO_2 (9.625 mA/cm^2) as the passivation layer reduces surface recombination, preserving more carriers and enabling a stronger photocurrent. Both-sided SiO_2 wafers may have slightly lower current densities (7.542 mA/cm^2), which may be affected by the limitation of the charge carrier population available for conduction.

Furthermore, the V_{oc} of undoped Ag paste samples was relatively low, with single-sided and both-sided passivated wafers exhibiting V_{oc} values of 0.35 V and 0.487 V, respectively. The both-sided passivated wafers will likely exhibit a higher V_{oc} because the SiO_2 layer minimizes recombination, thereby preserving the carrier population. This preservation of carriers supports a higher potential difference across the junction when no external load is applied. For one-sided SiO_2 exhibits a lightly lower V_{oc} than fully passivated wafers, as the unpassivated side introduces more opportunities for recombination, reducing the net carrier concentration and thus the potential difference.

Fully passivated wafers will generally exhibit higher FFs (0.303) because reduced surface recombination leads to less current loss and a better preservation of charge carriers. This results in a more efficient power output, maximizing the squareness of the I-V curve. For one-sided passivated wafers, the FF may be slightly lower (0.289) than that of fully passivated wafers due to potential increases in series resistance or recombination on the unpassivated side. The paste's quality and the nature of the contact impact the FF significantly. If the Ag paste is well optimized, it provides good ohmic contact, minimizing series resistance (Batchu *et al*., 2015; Unsur *et al*., 2015). However, if the contact introduces high resistance or leads to shunt paths, the FF can decrease, as more power is lost.

The fill factor (FF) is influenced by the contact resistance, recombination rates, and the quality of the Ag-P interface (Qi & Wang, 2013). Phosphorus doping enhances carrier concentration, which helps in achieving a more defined and higher FF by improving conductivity. In this paper, the Ag-P paste plays a significant role in ensuring strong ohmic contact, minimizing series resistance and reducing the chances of shunting pathways. The FF varied across wafer types, with the highest recorded FF on textured wafers (0.331) and lower FF values for both single-sided SiO_2 (0.298) and fully passivated wafers (0.251). The increase in FF for textured wafers may be due to improved contact quality and the effectiveness of in-situ doping, though surface roughness may introduce some recombination. The overall FF improvement for phosphorus-doped samples over undoped samples indicates that in-situ doping enhanced charge collection and reduced resistive losses.

The Ag-P paste significantly enhanced efficiency, with single-sided passivated wafers achieving an efficiency of 1.65%. This efficiency boost can be attributed to better carrier generation and collection due to phosphorus doping, which enhances the p-n junction's effectiveness and reduces recombination (Nawaz *et al*., 2020; Xu *et al*., 2023). However, fully passivated samples showed slightly lower efficiency (0.15%), possibly due to increased resistance or suboptimal contact formation with dual oxide layers.

Phosphorus doping significantly influences the results, as evident in the Ag-P paste samples. The oxide-passivated configuration, particularly with one-sided passivation, achieves a V_{oc} of 0.533 V and J_{sc} of 10.4 mA/cm², resulting in a substantially improved efficiency of 1.65%. However, in configurations such as planar and textured surfaces without oxide passivation, the doped paste shows limited improvement in V_{oc} and J_{sc}, particularly for the planar configuration, which is near-zero values, indicating ineffective current generation and charge collection.

According to Table 1, the water-based H_3PO_4 shows the highest efficiency of 5.67% as compared with undoped and Ag-P doped silicon solar cells, suggesting better emitter quality and charge collection. Undoped Ag-based paste silicon solar cells exhibit significantly lower performance. The one side O_2 treated sample has efficiency lower than 1% due to poor charge transport. So, it was reflected in a very low V_{OC} of 0.35V and JSC of 9.625 mA/cm^2. However, the sample with both sides O_2 shows an improvement in V_{OC} of 0.487 V but suffers from a much lower J_{SC} of 7.542 mA/cm^2, leading to only 1.11% of overall efficiency. Thus, undoped silicon solar cells with one side and both side O_2 suggest that oxygen treatment negatively impacts carrier mobility and junction quality which is potentially introducing defects or oxidation at the metallic contact interfaces.

Other than that, the performance of Ag-P dopant pastes and undoped Ag in Si solar cells varies significantly due to the differences in doping effects and electrical properties. The Ag-P with one side O_2 exhibits a higher V_{OC} of 0.533 V and J_{SC} of 10.4 mA/cm^2 compared to overall undoped Ag paste. This improvement is due to phosphorus doping enhancing the emitter properties and reducing recombination losses near interfaces. The lowest-performing of silicon solar cells with below 0.5% are achieved from Ag-P on planar, textured, and both side O_2, suggesting excessive oxygen treatment in Ag-P paste that will enhance resistive losses or defect formation.

Water-based H_3PO_4 as an emitter outperforms both Ag-P doped and undoped Ag in silicon solar cells. While Ag-P paste improves over undoped paste, it still falls far behind H_3PO_4-based emitters in overall performance. This highlights the

Table 1
Silicon solar cell parameters for undoped and phosphorus-doped Ag-based (Ag-P) paste

Samples		Voc (V)	Jsc (mA/cm2)	Fill factor	Efficiency (%)
Commercial		0.609	32.56	0.656	13
Water-based H_3PO_4 as emitter on Si		0.489	23.44	0.4943	5.67
Undoped (Ag-based) paste	One side O_2	0.35	9.625	0.289	0.97
	Both side O_2	0.487	7.542	0.303	1.11
Phosphorus-doped Ag-based (Ag-P) paste	Planar	0.028	0.14	0	0
	Textured	0.345	3.33	0.331	0.37
	One side O_2	0.533	10.4	0.298	1.65
	Both side O_2	0.562	1.09	0.251	0.15

effectiveness of water-based phosphorus diffusion over paste-based doping methods in achieving higher solar cell efficiency.

Overall, the Ag-based pastes were applied through a screen-printing process onto different wafer types: planar, textured, doped, fully passivated, and one-sided SiO_2 wafers. However, for the planar and textured wafers, no current-voltage (I-V) characteristics were observed because these wafers lacked a p-n junction layer necessary for photovoltaic activity. The absence of a p-n junction means that there is no electric field to separate the photo-generated electron-hole pairs. Without this separation, charge carriers recombine instead of flowing as an electric current, preventing light energy from being converted into usable electrical power. Therefore, wafers without a p-n junction cannot generate a measurable I-V response, confirming the essential role of the junction in solar cell operation (Hirst, 2012; Kitai, 2019).

In semiconductor materials, carrier mobility indicates how quickly the charge carrier (electron or holes) can move through the material under an electric field. For wafers with Ag-based paste, the mobility will depend largely on surface properties such as roughness in textured wafers and interface characteristics in passivated wafers (Mori *et al*., 2020; Poncé *et al*., 2020). Passivation layers like SiO_2 typically enhance mobility by reducing surface recombination, allowing for more efficient movement of carriers, as they mitigate the interaction of carriers with defects on the wafer's surface (Bonilla *et al*., 2017; Muduli & Kale, 2023). In textured and planar wafers with Ag-P paste but no p-n junction, mobility may be limited, as these surfaces lack the built-in field that aids in charge separation and movement.

In phosphorus-doped, passivated wafers, carrier mobility is expected to improve due to two factors which is phosphorus doping enhances the carrier density, potentially allowing more carriers to respond to the electric field and the passivation layer reduces surface defects, allowing carriers to move with less obstruction (Salemi *et al*., 2011; Xing *et al*., 2020). This effect is especially pronounced in fully passivated wafers, where the passivation reduces scattering sites that could hinder mobility.

Phosphorus doping significantly increases the carrier concentration, as the doping process introduces additional carriers, specifically electrons, which enhance the conductivity of the wafer. High carrier concentration is beneficial because it increases the likelihood of charge carriers being available to conduct current, which is essential for efficient device operation (Hooten *et al*., 2012). For planar and textured wafers without a p-n junction, the carrier concentration alone does not significantly impact current generation, as there is no mechanism to efficiently separate electron-hole pairs.

Recombination is the process where electrons and holes neutralize each other, releasing energy as heat. High recombination rates result in fewer carriers being available for conduction, reducing the efficiency of the wafer (Bonilla *et al*., 2017; Bonilla & Wilshaw, 2014). In phosphorus-doped, passivated wafers, the passivation layer (often made of SiO_2) reduces surface recombination by mitigating the availability of defect states where recombination can occur. This reduction in recombination is significant, as it preserves a larger proportion of carriers, which then contributes to higher photocurrents. Fully passivated wafers exhibit the lowest recombination rates, while wafers with only one-sided passivation may experience more recombination at the unpassivated side, although still improved compared to unpassivated surfaces.

3.3 Quantum Efficiency

Quantum efficiency (QE) is a critical parameter in silicon cells as it measures the cell's ability to convert incident photons into charge carriers. Specifically, external quantum efficiency (EQE) assesses the fraction of photons converted into electrical current, factoring in reflection and absorption losses, while internal quantum efficiency (IQE) considers only the absorbed photons (Kaya & Hajimirza, 2018; W. J. Yang *et al*., 2008). High QE values across a broad spectrum indicate efficient light absorption and minimal recombination losses, which are crucial for maximizing energy conversion efficiency and overall solar cell performance.

The EQE curves in Figure 8 show the different solar cell configurations, which are Ag-based with one side and both side oxidation and Ag-P based with one side and both side oxidation. The graph shows notable variation across the spectrum. At a shorter wavelength (200 – 400 nm), where surface recombination dominates, the cell with double-sided oxygen passivation demonstrates higher EQE values compared to single-sided passivation. This is expected, as double-sided passivation significantly reduces surface recombination, allowing for a more efficient collection of charge carriers generated near the surface.

In the visible range (400 – 800 nm), the EQE remains relatively high for all configurations, reflecting efficient absorption in the active layer of the silicon solar cells. However, the Ag-P paste cells may exhibit slightly improved performance compared to purely Ag-based paste cells due to the combined effects of improved contact conductivity and reduced surface recombination through phosphoric acid treatment. The EQE declines at a longer wavelength range (800 – 1200 nm), where light absorption is less efficient in silicon due to the indirect bandgap nature of the material. However, double-sided passivation still offers an advantage by minimizing recombination in bulk, leading to a slower drop-off in EQE compared to single-sided passivated cells.

On the other hand, internal quantum efficiency (IQE) reflects the intrinsic efficiency of the device, excluding optical losses. As expected, the IQE curves in Figure 9 show are higher across the whole wavelength spectrum than EQE, since reflection and transmission losses are not considered. The IQE performance across different device structures reveals the impact of recombination mechanisms. In the short wavelength range, the higher IQE values for double-sided passivation demonstrate that surface recombination is well mitigated. The fact that IQE remains relatively high in the near-infrared range (above 800 nm) suggests effective control over bulk recombination, possibly aided by better quality front contacts from the silver-doped paste and passivation.

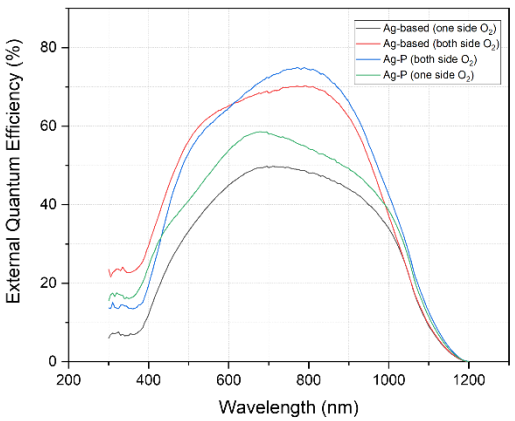

Fig 8 External quantum efficiency for undoped and phosphorus-doped Ag-based (Ag-P) paste

On the other hand, internal quantum efficiency (IQE) reflects the intrinsic efficiency of the device, excluding optical losses. As expected, the IQE curves in Figure 9 show are higher across the whole wavelength spectrum than EQE, since reflection and transmission losses are not considered. The IQE performance across different device structures reveals the impact of recombination mechanisms. In the short wavelength range, the higher IQE values for double-sided passivation demonstrate that surface recombination is well mitigated. The fact that IQE remains relatively high in the near-infrared range (above 800 nm) suggests effective control over bulk recombination, possibly aided by better quality front contacts from the silver-doped paste and passivation.

Ag-based pastes primarily improve the front's electrical contact, enhancing charge collection, especially in the visible to near-infrared regions (400 – 1200 nm). This results in higher EQE values in these ranges, as fewer carriers are lost due to poor contact. However, the absence of phosphoric acid means that the paste is less effective at reducing surface recombination losses, particularly in the UV region (200 – 400 nm), where surface recombination plays a significant role. As a result, Ag-based cells might show relatively lower EQE and IQE at shorter wavelengths.

The addition of phosphoric acid in the Ag-P paste introduces passivation effects that help reduce both surface and contact recombination losses. This is especially beneficial at shorter wavelength, where surface recombination is dominant. As a result, the Ag-P based cells are expected to show higher EQE and IQE in the blue-light region (200 – 400 nm), as the improved passivation and contact quality led to more efficient collection of short-wavelength photons. In the mid to long wavelength range (400 – 1200 nm), the Ag-P paste further contributes to maintaining higher efficiency by minimizing recombination losses throughout the device, leading to higher IQE and, subsequently, EQE in these ranges.

The light-current-voltage (IV) and quantum efficiency (QE) graphs in this study exhibit an unsynchronized relationship, indicating that while improvements in current density and efficiency are observed, these enhancements do not translate uniformly across all operational parameters. This difference is observed when comparing the IV characteristics with the external and internal quantum efficiency (EQE and IQE) responses, particularly for phosphorus-doped Ag-based (Ag-P) paste samples.

The IV graph shows an increase in J_{sc} and efficiency for certain configurations, especially with phosphorus doping on one-side oxide-passivated wafers. This suggests that doping improves the charge carrier collection by reducing surface recombination, which is reflected in the increased J_{sc} values for these samples. However, the QE graph, which provides insight into the spectral response of the solar cells, reveals inconsistencies. Although the QE values should theoretically align with the J_{sc} improvements observed in the IV graph, they show less evident gains or even declining efficiency in specific wavelength regions, particularly in the UV-visible spectrum.

These inconsistencies between the IV and QE graphs may stem from several underlying factors. One potential factor is surface recombination, which can be mitigated to a certain extent by phosphorus doping, thus enhancing J_{sc} as observed in the IV results. However, the QE graphs indicate that surface recombination may still impact specific wavelength ranges, particularly those associated with short-wavelength light, where surface passivation plays a crucial role. This effect may reduce the overall QE response, leading to an incomplete translation of the J_{sc} improvements from IV measurements to enhanced spectral response in QE.

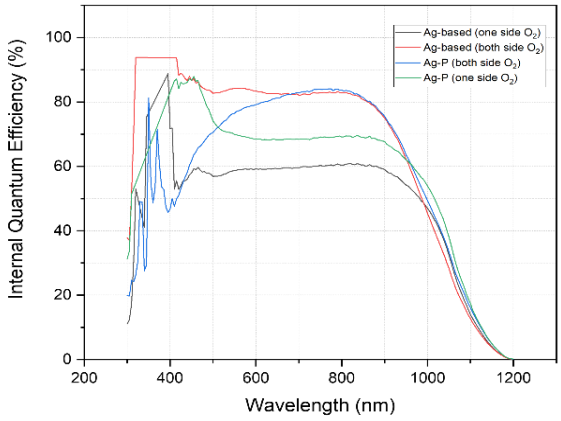

Fig 9 Internal quantum efficiency for undoped and phosphorus-doped Ag-based (Ag-P) paste

Furthermore, the lack of synchronization could also be attributed to the limited depth of phosphorus diffusion achieved with the Ag-P paste. While the IV graph reflects general improvements in the current generation due to the doped contacts, the QE response might be hindered by suboptimal doping profiles, which could restrict charge carrier collection efficiency across the entire light spectrum. This suggests that while phosphorus doping in the Ag-P paste enhances general electrical characteristics, further optimization in doping depth and surface passivation may be required to achieve consistent performance gains across both IV and QE measurements.

Other than that, the IQE and EQE measurements were taken for Ag-P screen-printed on Si wafers across different wavelengths. The results showed that this sample achieved higher IQE (80-83%) and EQE (63-73%) in the 650-900 nm wavelength range compared to the other samples. The superior performance of Ag-P on Si wafers is likely due to better carrier collection and reduced recombination losses. The phosphorus doping improves conductivity and enhances the passivation effect, minimizing surface defects. Additionally, this wavelength range corresponds to strong absorption in silicon, ensuring efficient photon-to-electron conversion.

Overall, the findings show that phosphorus-doped Ag-based (Ag-P) paste performs differently depending on how the surface is treated. The planar sample had the worst performance, meaning it did not conduct electricity well. Texturing helped slightly by improving light absorption. One-side oxygen (O_2) treatment gave the best results, increasing voltage and current flow, leading to better efficiency. However, both-side O_2 treatment caused too much oxidation, which reduced current flow and overall efficiency. This suggests that controlled oxygen treatment improves performance, but too much oxidation can block the movement of electrical charges, reducing the effectiveness of the solar cell.

Other than that, the Ag-P paste enables an in-situ process for simultaneous metal contact formation and emitter junction doping under contacts in silicon solar cells. This process involves phosphorous diffuses from the paste at high temperature into Si, forming an n^+ emitter layer while Ag establishes low-resistance ohmic contacts. Thus, this in-situ approach eliminates separate doping and metallization steps, simplifying fabrication process. Such that, it is suitable to be implemented into fabrication process of latest silicon solar cells technology like tunnel oxide passivated contact (TOPCon).

Furthermore, this process can be one of the solutions in eliminating alignment process and photolithography process in fabricating back contact silicon solar cells by using traditional screen-printing process for metallization and emitter formation.

3.4 Limitations and future recommendations

This study has several limitations. Firstly, some samples, such as planar and textured wafers, did not have a p-n junction, which is essential for charge separation and current generation. Additionally, the research only examined two Ag-P concentrations (5% and 10%) and two annealing times (10s and 40s), which may not be enough to determine the best processing conditions. The study also focused only on one-sided SiO_2 passivation, while other passivation techniques might offer better performance. Moreover, contact resistance and paste uniformity could have affected measurement accuracy. To improve this research, future studies should test a wider range of Ag-P concentrations and annealing conditions. Long-term stability tests should be conducted under real-world conditions. Advanced characterization methods, such as TEM and XPS, can provide a better understanding of material behavior. Finally, applying Ag-P to fully fabricated solar cells will help evaluate its commercial viability.

4. Conclusion

In conclusion, this study demonstrates the potential of phosphorus-doped silver (Ag-P) paste as an effective alternative for enhancing the electrical performance of p-type silicon solar cells through in-situ doping and contact formation. By integrating phosphorus doping into the silver paste, the Ag-P paste addresses critical limitations in traditional screen-printing methods by simultaneously forming the emitter region and the metallic contacts, simplifying the fabrication process and reducing production costs. This study found that 10% Ag-P paste with 40s annealing improved contact formation and efficiency. One-sided SiO_2 passivation reduced recombination, enhancing performance. Future research should explore alternative passivation, Ag-P concentrations, and long-term stability. The experimental results indicate that the Ag-P paste significantly improves J_{sc}, quantum efficiency, and overall conversion efficiency, particularly in configurations with single-sided silicon dioxide passivation. Enhanced quantum efficiency, especially in the UV-visible range, was achieved by effectively mitigating surface recombination losses, leading to improved charge carrier collection. These findings could help develop more efficient, cost-effective solar cells for sustainable energy applications. Future research could explore alternative dopant formulations, optimized firing profiles, and compatibility with next-generation silicon architectures to further enhance efficiency and long-term stability.

Acknowledgments

This work has been carried out with the support of the Laboratory Research Grant Scheme (LRGS/1/2019/UKM-UKM/6/1). In addition, I want to express many thanks to Dr. Saleem H. Zaidi from Gratings Incorporated, Albuquerque, New Mexico, USA for collaboration and guidance in completing the whole process of the theoretical and experimental works.

Author Contributions: N.A.M.S.: Conceptualization, methodology, formal analysis, writing-original draft, A.R.M.R.; writing-review and editing, methodology, Z.F.M.A.; writing-review, and editing, K.S.; project administration, validation, M.A.I.; supervision, writing-review and editing, resources, project leader. All authors have read and agreed to the published version of the manuscript.

Funding: This research was funded by Laboratory Research Grant Scheme (LRGS/1/2019/UKM-UKM/6/1).

Conflicts of Interest: The authors declare no conflict of interest.

References

Abid, Z., Wahad, F., Gulzar, S., Ashiq, M. F., Aslam, M. S., Shahid, M., Altaf, M., & Ashraf, R. S. (2023). Solar Cell Efficiency Energy Materials. *Fundamentals of Solar Cell Design*, 271–315. https://doi.org/10.1002/9781119725022.ch10

Akter, N., Hossion, A., & Amin, N. (2022). *Fabrication of Oxide Passivated and Antireflective Thin Film Coated Emitter Layer in Two Steps for the Application in Photovoltaic*. *09*(03).

Alamri, H. R., Rezk, H., Abd-elbary, H., & Ziedan, H. A. (2020). Experimental Investigation to Improve the Energy Efficiency of Solar PV Panels Using Hydrophobic. *Coatings*, *10*(5).

Andreani, L. C., Bozzola, A., Kowalczewski, P., Liscidini, M., & Redorici, L. (2019). Silicon solar cells: Toward the efficiency limits. *Advances in Physics: X*, *4*(1). https://doi.org/10.1080/23746149.2018.1548305

Antoniadis, H. (2011). *High Efficiency , Low Cost Solar Cells Manufactured Using ' Silicon Ink ' on Thin Crystalline Silicon Wafers High Efficiency , Low Cost Solar Cells Manufactured Using ' Silicon Ink ' on Thin Crystalline Silicon Wafers* (Issue October 2009). https://docs.nrel.gov/docs/fy11osti/50824.pdf

Basher, M. K., Hossain, M. K., & Akand, M. A. R. (2019). Effect of surface texturization on minority carrier lifetime and photovoltaic performance of monocrystalline silicon solar cell. *Optik*, *176*(July 2018), 93–101. https://doi.org/10.1016/j.ijleo.2018.09.042

Batchu, K., Unsur, V., Ebong, A., Member, S., Batchu, K., Charlotte, U. N. C., Charlotte, U. N. C., Paste, K. W.--A., & Resistance, C. (2015). The Impact of Ag Particle Size and Rapid Thermal Processing Belt Speed on Contact Resistance of a Silicon Solar Cell. *IEEE*, 43–46.

Battaglia, C., Cuevas, A., & De Wolf, S. (2016). High-efficiency crystalline silicon solar cells: Status and perspectives. *Energy and Environmental Science*, *9*(5), 1552–1576. https://doi.org/10.1039/c5ee03380b

Bonilla, R. S., Hoex, B., Hamer, P., & Wilshaw, P. R. (2017). Dielectric surface passivation for silicon solar cells: A review. *Physica Status Solidi (A) Applications and Materials Science*, *214*(7), 1–30. https://doi.org/10.1002/pssa.201700293

Bonilla, R. S., & Wilshaw, P. R. (2014). A technique for field effect surface passivation for silicon solar cells A technique for field effect surface passivation for silicon solar cells. *Applied Physics Letters*, *104*, 232903. https://doi.org/10.1063/1.4882161

Chaudhary, A., Hos, J., Lossen, J., Huster, F., Kopecek, R., Van Swaaij, R., & Zeman, M. (2022). Screen Printed Fire-Through Contact Formation for Polysilicon-Passivated Contacts and Phosphorus-Diffused Contacts. *IEEE Journal of Photovoltaics*, *12*(2), 462–468. https://doi.org/10.1109/JPHOTOV.2022.3142135

Chaudhary, A., Hoß, J., Lossen, J., van Swaaij, R., & Zeman, M. (2021). Advancement in screen printed fire through silver paste metallisation of polysilicon based passivating contacts. *AIP Conference Proceedings*, *2367*(June). https://doi.org/10.1063/5.0055978

Chen, C., Ran, C., Yao, Q., Wang, J., Guo, C., Gu, L., Han, H., Wang, X., Chao, L., Xia, Y., & Chen, Y. (2023). Screen-Printing Technology for Scale Manufacturing of Perovskite Solar Cells. *Advanced Science*, *10*(28). https://doi.org/10.1002/advs.202303992

Chen, Y. L., Lu, G. L., Zhong, S. H., & Shen, W. Z. (2016). SiO 2 Passivation Layer Grown by Liquid Phase Deposition for N-type Bifacial Silicon Solar Cells. *MATEC Web of Conferences*, *04008*(67).

Chowdhury, S., Kumar, M., Dutta, S., Park, J., Kim, J., Kim, S., Ju, M., Kim, Y., Cho, Y., Cho, E.-C., & Yi, J. (2019). High-efficiency Crystalline Silicon Solar Cells: A Review. *New & Renewable Energy*, *15*(3), 36–45. https://doi.org/10.7849/ksnre.2019.3.15.3.036

Dou, B., Jia, R., Xing, Z., Yao, X., Xiao, D., Jin, Z., & Liu, X. (2021). Enhanced performance of nanotextured silicon solar cells with excellent light-trapping properties. *Photonics*, *8*(7). https://doi.org/10.3390/photonics8070272

Eon, D., Umezawa, H., Iwasaki, T., Murooka, T., Hatano, M., Araujo, D., Pernot, J., Kawarada, H., Kato, H., Makino, T., & Koizumi, S. (2018). Device formation and the characterizations. In *Power Electronics Device Applications of Diamond Semiconductors*. https://doi.org/10.1016/B978-0-08-102183-5.00005-4

Gaubert, P., & Teramoto, A. (2017). Carrier Mobility in Field-Effect Transistors. In *Intech* (Vol. 11, p. 13). https://www.intechopen.com/books/advanced-biometric-technologies/liveness-detection-in-biometrics

Glatthaar, R., Huster, F., Okker, T., Cela Greven, B., Seren, S., Hahn, G., & Terheiden, B. (2022). Contact Formation of Silver Paste and Atmospheric Pressure Chemical Vapor Deposition (n) Poly-Silicon Passivating Contacts on Planar and Textured Surfaces. *Physica Status Solidi (A) Applications and Materials Science*, *219*(24), 1–8. https://doi.org/10.1002/pssa.202200501

Glunz, S. W., & Feldmann, F. (2018). SiO2 surface passivation layers – a key technology for silicon solar cells. *Solar Energy Materials and Solar Cells*, *185*(February), 260–269. https://doi.org/10.1016/j.solmat.2018.04.029

Goodrich, A., Hacke, P., Wang, Q., Sopori, B., Margolis, R., James, T. L., & Woodhouse, M. (2013). A wafer-based monocrystalline silicon photovoltaics road map: Utilizing known technology improvement opportunities for further reductions in manufacturing costs. *Solar Energy Materials and Solar Cells*, *114*, 110–135. https://doi.org/10.1016/j.solmat.2013.01.030

Hamzavy, B. T., & Bradley, alexander Z. (2013). Safety and Performance Analysis of a Commercial Photovoltaic Installation. *Proceedings of SPIE*, *8825*, 1–7. https://doi.org/10.1117/12.2023406

Hirst, L. C. (2012). Principles of Solar Energy Conversion. *Comprehensive Renewable Energy*, *1*, 293–313.

Hooten, N. C., Edmonds, L. D., Bennett, W. G., Ahlbin, J. R., Dodds, N. A., Reed, R ASchrimpf, R. D., & Weller, R. A. (2012). The Significance of High-Level Carrier Generation Conditions for Charge Collection in Irradiated Devices. *IEEE Transaction on Nuclear Science*, *59*(6), 2710–2721.

Kaya, M., & Hajimirza, S. (2018). Rapid Optimization of External Quantum Efficiency of Thin Film Solar Cells Using Surrogate Modeling of Absorptivity. *Scientific Reports*, *8*(1), 1–9. https://doi.org/10.1038/s41598-018-26469-3

Kim, M. S., Lee, J. H., & Kwak, M. K. (2020). Review: Surface Texturing Methods for Solar Cell Efficiency Enhancement. *International Journal of Precision Engineering and Manufacturing*, *21*(7), 1389–1398. https://doi.org/10.1007/s12541-020-00337-5

Kitai, A. (2019). p – n Junction Solar Cells. In *Principles of Solar Cells, LEDs and related devices: The role of the PN junction* (second edi, pp. 202–257). John Wiley & Sons Ltd.

Kulushich, G., Zapf-Gottwick, R., Nguyen, V. X., & Werner, J. H. (2012). Role of phosphorus in contact formation on silicon solar cells. *Physica Status Solidi - Rapid Research Letters*, *6*(9–10), 370–372. https://doi.org/10.1002/pssr.201206298

Lan, C. W., Hsu, C., & Nakajima, K. (2015). Multicrystalline Silicon Crystal Growth for Photovoltaic Applications. In *Handbook of Crystal Growth: Bulk Crystal Growth: Second Edition* (Second Edi, Vol. 2). Elsevier B.V. https://doi.org/10.1016/B978-0-444-63303-3.00010-9

Larionova, Y., Turcu, M., Reiter, S., Brendel, R., Tetzlaff, D., Krugener, J., Wietler, T., Hohne, U., Kahler, J., & Peibst, R. (2017). On the recombination behavior of p-type polysilicon on oxide junctions deposited by different methods on textured and planar surfaces. *Physica Status Solidi (A) Applications and Materials Science*, *1700058*, 1–5. https://doi.org/10.1002/pssa.201700058

Lee, S.-H., & Heo, S.-Y. (2017). *Silver paste composition for forming an electrode, and silicon solar cell using same*.

Li, H., Kim, K., Hallam, B., Hoex, B., Wenham, S., & Abbott, M. (2017). POCl3 diffusion for industrial Si solar cell emitter formation. *Frontiers in Energy*, *11*(1), 42–51. https://doi.org/10.1007/s11708-016-0433-7

Lorenz, A., Linse, M., Frintrup, H., Jeitler, M., Mette, A., Lehner, M., Greutmann, R., Brocker, H., König, M., Erath, D., & Clement, F. (2018). Screen Printed Thick Film Metallization of Silicon Solar Cells - Recent Developments and Future Perspectives. *35th European Photovoltaic Solar Energy Conference and Exhibition*, *September*, 819–824. https://userarea.eupvsec.org/proceedings/35th-EU-PVSEC-2018/2DV.3.65/

Mandal, N. C., Biswas, S., Acharya, S., Panda, T., Sadhukhan, S., Sharma, J. R., Nandi, A., Bose, S., Kole, A., Das, G., Maity, S., Chaudhuri, P., & Saha, H. (2020). Materials Science in Semiconductor Processing Study of the properties of SiO x layers prepared by different techniques for rear side passivation in TOPCon solar cells. *Materials Science in Semiconductor Processing*, *119*(June), 105163. https://doi.org/10.1016/j.mssp.2020.105163

Meier, D. L., Davis, H. P., Garcia, R. A., Jessup, J. A., & Carroll, A. F. (2000). Self-doping contacts to silicon using silver coated with a dopant source. *Conference Record of the IEEE Photovoltaic Specialists Conference*, *2000-Janua*, 69–74. https://doi.org/10.1109/PVSC.2000.915755

Mohd Ahir, Z. F., Sepeai, S., & H. Zaidi, S. (2018). Optimization of Phosphoric Acid-Based Emitter Formation on Silicon Wafer. *Jurnal Kejuruteraan*, *SI1*(3), 9–14. https://doi.org/10.17576/jkukm-2018-si1(3)-02

Mohd Rais, A. R., Mohd Sinin, N. A., Sepeai, S., Ibrahim, M. A., Zaidi, S. H., & Sopian, K. (2022). Analysis of Spectral Transmission in Si Solar Cell with Pyramidal Texturization by Using PC3S Simulation. *Silicon*. https://doi.org/10.1007/s12633-021-01373-0

Mori, K., Samata, S., Mitsugi, N., Teramoto, A., Kuroda, R., Suwa, T., Hashimoto, K., & Sugawa, S. (2020). Influence of silicon wafer surface roughness on semiconductor device characteristics. *Japanese Journal of Applied Physics*, *59*, SMMB06.

Muduli, sakti prasanna, & Kale, P. (2023). State-of-the-art passivation strategies of c-Si for photovoltaic applications: A review. *Materials Science in Semiconductor Processing*, *154*, 107202. https://doi.org/10.1016/j.mssp.2022.107202

Nawaz, A., Tahir, S., Ali, A., Arshad, M. I., Mahmood, K., Siraj, S., & Muddassir, Y. (2020). Effect of phosphorous/boron doping profile differences on the performance of silicon solar cells. *Journal of Ovonic Research*, *16*(1), 63–70.

Oh, K. suk, Bae, S., Lee, K. jin, Kim, D., & Chan, S. il. (2019). Mitigation of potential-induced degradation (PID) based on anti-reflection coating (ARC) structures of PERC solar cells. *Microelectronics Reliability*, *100–101*(May), 113462. https://doi.org/10.1016/j.microrel.2019.113462

Poncé, S., Li, W., Reichardt, S., & Giustino, F. (2020). First-principles calculations of charge carrier mobility and conductivity in bulk semiconductors and two-dimensional materials. *Reports on Progress in Physics*, *83*(3). https://doi.org/10.1088/1361-6633/ab6a43

Porter, L. M., Teicher, A., & Meier, D. L. (2002). Phosphorus-doped, silver-based pastes for self-doping ohmic contacts for crystalline silicon solar cells. *Solar Energy Materials and Solar Cells*, *73*(2), 209–219. https://doi.org/10.1016/S0927-0248(01)00126-X

Proul, A. (2023). Understanding the p-n Junction. *Solar Cells: Resource for the Secondary Science Teacher*, 13–24.

Qi, B., & Wang, J. (2013). Fill factor in organic solar cells. *Physical Chemistry Chemical Physics*, *15*(23), 8972–8982. https://doi.org/10.1039/c3cp51383a

Rahman, M. Z., & Khan, S. I. (2012). Advances in surface passivation of c-Si solar cells. *Mater Renew Sustain Energy*, 1–11. https://doi.org/10.1007/s40243-012-0001-y

Razeghi, M. (2009). PN and Metal-Semiconductor Junctions. In *Fundamentals of Solid State Engineering*. https://doi.org/10.1007/978-0-387-92168-6_9

Rujhan, A., Rais, M., Aqidah, N., Sinin, M., Rohaizar, M. H., Ibrahim, M. A., Sopian, K., & Sepeai, S. (2024). Phosphorus Activation via Screen Printing Ag / P on Thermally Grown SiO 2 Layer as Passivating Contact on n-Si. *Journal of Physical Science*, *35*(3), 65–80.

Salemi, S., Potbhare, A. A. S., Lelis, A., & Goldsman, N. (2011). The Effects of Different Silicon Carbide – Silicon Dioxide Interface Passivations on Transition Region Mobility and Transport. *Int. Semiconductor Devuice Research Symposium*, 10–11.

Savadogo, M., Soro, B., Konate, R., Sourabié, I., Zoungrana, M., Zerbo, I., & Joseph Bathiebo, D. (2020). Temperature Effect on Light Concentration Silicon Solar Cell's Operating Point and Conversion Efficiency. *Smart Grid and Renewable Energy*, *11*(05), 61–72. https://doi.org/10.4236/sgre.2020.115005

Sepeai, S., Sulaiman, M. Y., & Sopian, K. (2011). Optimization of rapid thermal firing on silver metal contact for crystalline silicon solar cells. *AIP Conference Proceedings*, *1328*(2011), 196–198. https://doi.org/10.1063/1.3573727

Serenelli, L., Martini, L., Menchini, F., Izzi, M., & M. Tucci. (2023). Open circuit voltage reduction due to recombination at the heterojunction solar cell edge. *Solar Energy*, *258*, 2–7. https://doi.org/10.1016/j.solener.2023.04.027

Shanmugam, V., Cunnusamy, J., Khanna, A., Basu, P. K., Zhang, Y., Chen, C., Stassen, A. F., Boreland, M. B., Mueller, T., Hoex, B., & Aberle, A. G. (2014). Electrical and microstructural analysis of contact formation on lightly doped phosphorus emitters using thick-film ag screen printing pastes. *IEEE Journal of Photovoltaics*, *4*(1), 168–174. https://doi.org/10.1109/JPHOTOV.2013.2291313

Shanmugam, V., Khanna, A., Basu, P. K., Aberle, A. G., Mueller, T., & Wong, J. (2016). Impact of the phosphorus emitter doping profile on metal contact recombination of silicon wafer solar cells. *Solar Energy Materials and Solar Cells*, *147*, 171–176. https://doi.org/10.1016/j.solmat.2015.12.006

Sheng, J., Ma, Z., Cai, W., Ma, Z., Ding, J., Yuan, N., & Zhang, C. (2019). Impact of phosphorus diffusion on n-type poly-Si based passivated contact silicon solar cells. *Solar Energy Materials and Solar Cells*, *203*(March), 110120. https://doi.org/10.1016/j.solmat.2019.110120

Sinin, N. A. M., Rais, A. R. M., Sopian, K., & Ibrahim, M. A. (2023). The concentration factor on the mixture of Ag paste and H3 PO4 solution as a dopant paste for contact formation in silicon solar cells. *Journal of Ovonic Research*, *19*(6), 681–694. https://doi.org/10.15251/JOR.2023.196.681

Skromme, B. J. (2003). Junctions and Barriers. *Encyclopedia of Materials: Science and Technology*, 1–12. https://doi.org/10.1016/b0-08-043152-6/01896-9

Sopian, K., Cheow, S. L., & Zaidi, S. H. (2017). An overview of crystalline silicon solar cell technology: Past, present, and future. *AIP Conference Proceedings*, *1877*(September). https://doi.org/10.1063/1.4999854

Sui, M., Chu, Y., & Zhang, R. (2021). A review of technologies for high efficiency silicon solar cells. *Journal of Physics: Conference Series*, *1907*(1). https://doi.org/10.1088/1742-6596/1907/1/012026

Tepner, S., & Lorenz, A. (2023). Printing technologies for silicon solar cell metallization : A comprehensive review. *Progress in Photovoltaics: Research and Applications*, *31*, 557–590. https://doi.org/10.1002/pip.3674

Tepner, S., Ney, L., Singler, M., Preu, R., & Pospischil, M. (2021). A model for screen utility to predict the future of printed solar cell metallization. *Nature*, *11*, 1–13. https://doi.org/10.1038/s41598-021-83275-0

Thibert, S., Jourdan, J., Bechevet, B., Chaussy, D., Reverdy-bruas, N., & Beneventi, D. (2014). Influence of silver paste rheology and screen parameters on the front side metallization of silicon solar cell. *Materials Science in Semiconductor Processing*, *27*, 790–799. https://doi.org/10.1016/j.mssp.2014.08.023

Tripathi, B., Mahapatra, A., Verma, D., Kalam, A., Pandey, M. K., Trivedi, S., & Kumar, M. (2020). Electro-analytical comparison of commercial mono-crystalline silicon and PERC solar cells to maximize performance Electro-analytical comparison of commercial mono-crystalline silicon and PERC solar cells to maximize performance. *Engineering Research Express*, *2*, 040518. https://doi.org/10.1088/2631-8695/abc362

Turkay, D., Koroglu, C., & Yerci, S. (2019). Analysis of Field-Effect Passivation in Textured and Undiffused Silicon Surfaces. *Physical Review Applied*, *12*(3), 1. https://doi.org/10.1103/PhysRevApplied.12.034026

Unsur, V., Chowdhury, A., Chen, N., & Ebong, A. (2015). The Effects ofNano Ag Particles on Gridline Sintering for Silicon Solar Cells. *IEEE*, 1–5.

Wu, W., Roelofs, K. E., Subramoney, S., Lloyd, K., & Zhang, L. (2017). Role of aluminum in silver paste contact to boron-doped silicon emitters. *AIP Advances*, *7*(1). https://doi.org/10.1063/1.4974752

Wurfel, U., Cuevas, A., & Peter, W. (2015). Charge Carrier Separation in Solar Cells. *IEEE Journal of Photovoltaics*, *5*(1), 461–469.

Xing, B., Tu, Y., Yao, J., Niu, X., Yan, X., Liu, Y., Wu, X., Li, M., Guo, W., Sha, J., & Wang, Y. (2020). surface charge transfer doping and effect passivation of black phosphorus field effect transistor. *Journal of Materials Chemistry C*, 1–25. https://doi.org/10.1039/D0TC00740D

Xu, X., Wu, W., & Wang, Q. (2023). Efficiency Improvement of Industrial Silicon Solar Cells by the POCl3 Diffusion Process. *Materials*, *16*(5). https://doi.org/10.3390/ma16051824

Yang, P., Zeng, X., Xie, X., Zhang, X., Li, H., & Wang, Z. (2013). Improved open-circuit voltage of silicon nanowires solar cells by surface passivation. *RSC Advances*, *3*(47), 24971–24974. https://doi.org/10.1039/c3ra42823k

Yang, W. J., Ma, Z. Q., Tang, X., Feng, C. B., Zhao, W. G., & Shi, P. P. (2008). Internal quantum efficiency for solar cells. *Solar Energy*, *82*(2), 106–110. https://doi.org/10.1016/j.solener.2007.07.010

Yüce, C., Okamoto, K., Karpowich, L., Adrian, A., & Willenbacher, N. (2019). Non-volatile free silver paste formulation for front-side metallization of silicon solar cells. *Solar Energy Materials and Solar Cells*, *200*. https://doi.org/10.1016/j.solmat.2019.110040

Zanesco, I., Crestani, T., Moehlecke, A., & Ly, M. (2019). Analysis of different conductive pastes to form the contact with the boron back surface field in PERT silicon solar cells. *Materials Research Express*, *6*(11). https://doi.org/10.1088/2053-1591/ab4b99

Zhang, S., Yao, Y., Hu, D., Lian, W., Qian, H., Jie, J., Wei, Q., Ni, Z., Zhang, X., & Xie, L. (2019). Application of silicon oxide on high efficiency monocrystalline silicon PERC solar cells. *Energies*, *12*(6), 1–11. https://doi.org/10.3390/en12061168

Zhou, L., Bo, B., Yan, X., Wang, C., Chi, Y., & Yang, X. (2018). Brief Review of Surface Passivation on III-V Semiconductor. *Crystals*, *8*(226), 1–14. https://doi.org/10.3390/cryst8050226

Zhou, Y. (2013). *Eco- and Renewable Energy Materials* (Y. Zhou (ed.)). Springer Heidelberg New York Dordrecht London.

Zhuang, Y. F., Zhong, S. H., Liang, X. J., Kang, H. J., Li, Z. P., & Shen, W. Z. (2019). Application of SiO 2 passivation technique in mass production of silicon solar cells. *Solar Energy Materials and Solar Cells*, *193*(January), 379–386. https://doi.org/10.1016/j.solmat.2019.01.038